Pannotia's mantle signature: the quest for supercontinent identification

Philip J. Heron[1]*, J. Brendan Murphy[2], R. Damian Nance[3,4] and R. N. Pysklywec[5]

[1]Department of Earth Sciences, Durham University, Durham, DH1 3LE, UK

[2]Department of Earth Sciences, St. Francis Xavier University, Antigonish, Nova Scotia, B2G 2W5, Canada

[3]Department of Geological Sciences, Ohio University, Ohio, 45701, USA

[4]Department of Earth & Planetary Sciences, Yale University, Connecticut, 06511, USA

[5]Department of Earth Sciences, University of Toronto, Toronto, Ontario, M5S 3B1, Canada

PJH, 0000-0002-4813-0504

*Correspondence: heronphi@gmail.com

Abstract: A supercontinent is generally considered to reflect the assembly of all, or most, of the Earth's continental lithosphere. Previous studies have used geological, atmospheric and biogenic 'geomarkers' to supplement supercontinent identification. However, there is no formal definition of how much continental material is required to be assembled, or indeed which geomarkers need to be present. Pannotia is a hypothesized landmass that existed in the interval *c.* 0.65–0.54 Ga and was comprised of Gondwana, Laurentia, Baltica and possibly Siberia. Although Pannotia was considerably smaller than Pangaea (and also fleeting in its existence), the presence of geomarkers in the geological record support its identification as a supercontinent. Using 3D mantle convection models, we simulate the evolution of the mantle in response to the convergence leading to amalgamation of Rodinia and Pangaea. We then compare this supercontinent 'fingerprint' to Pannotian activity. For the first time, we show that Pannotian continental convergence could have generated a mantle signature in keeping with that of a simulated supercontinent. As a result, we posit that any formal identification of a supercontinent must take into consideration the thermal evolution of the mantle associated with convergence leading to continental amalgamation, rather than simply the size of the connected continental landmass.

The formation of supercontinent Pangaea (Fig. 1a) had a profound effect on the thermal evolution of the mantle. An increase in deep mantle upwelling and plume formation is thought to follow supercontinent formation (Gurnis 1988; Lowman and Jarvis 1993; Zhong and Gurnis 1993; Zhong *et al.* 2007; Li and Zhong 2009; Yoshida 2010; Heron and Lowman 2010; Yoshida 2013; Gamal El Dien *et al.* 2019), with large igneous provinces (LIPs) being the surface manifestations of such plumes (e.g. Yale and Carpenter 1998; Courtillot *et al.* 1999; Ernst *et al.* 2005; Ernst and Bleeker 2010; Sobolev *et al.* 2011). Additional 'geomarkers' (see Nance *et al.* 1986) have also been identified for supercontinent Pangaea, including global-scale orogenesis (Nance *et al.* 1988; Santosh 2010*a*; Condie 2011; Müller *et al.* 2013), crustal growth (Hawkesworth *et al.* 2010, 2016), the distribution of metamorphic belts (Brown 2007) and mineral deposits (Goldfarb *et al.* 2010), rapid climate swings (Hoffman *et al.* 1998; Strand 2012; Young 2012), major events in the evolution of life and the atmosphere (Lindsay and Brasier 2002; Santosh 2010*b*; Knoll 2013; Melezhik *et al.* 2013), biogeochemical cycles (Nance *et al.* 1986), and profound sea-level change (Worsley *et al.* 1984; Nance and Murphy 2013). Such geomarkers are interpreted as signals of supercontinent convergence leading to amalgamation and may be useful proxies for identifying the existence of previous supercontinents for which palaeocontinental reconstructions may be less refined (Nance and Murphy 2019).

Although their ages of amalgamation and break-up are still being refined, a number of pre-Pangaean supercontinents have been proposed (based on the identification of geomarkers in the geological record). Rodinia (Fig. 1b), with Laurentia at its centre, was formed by 1.1–0.9 Ga global-scale orogenesis (Dalziel 1991; Hoffman 1991; Moores 1991; Torsvik 2003; Li *et al.* 2004, 2008). It was fully assembled by *c.* 900 Ma and is believed to have rifted apart in two separate episodes (*c.* 0.85–0.70 Ga and *c.* 0.62–0.54 Ga) (Li *et al.* 2008, 2013; Li and Evans 2011). Earlier supercontinents include Nuna/Columbia (Hoffman 1997; Rogers and Santosh 2002) whose existence is most recently

From: Murphy, J. B., Strachan, R. A. and Quesada, C. (eds) 2020. *Pannotia to Pangaea: Neoproterozoic and Paleozoic Orogenic Cycles in the Circum-Atlantic Region*. Geological Society, London, Special Publications, **503**, https://doi.org/10.1144/SP503-2020-7

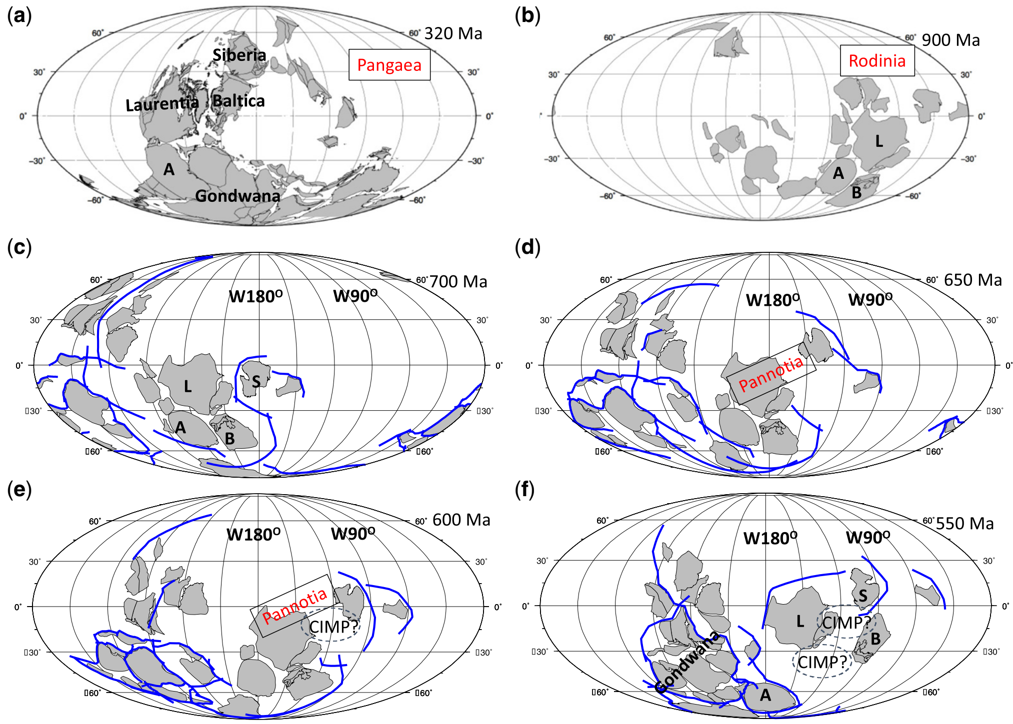

Fig. 1. Continental configurations at (**a**) 320 Ma (Matthews *et al.* 2016) for Pangaea formation; (**b**) 900 Ma (Merdith *et al.* 2017) for Rodinia formation; (**c**) 700 Ma (Merdith *et al.* 2017) for Pannotia amalgamation ; (**d**) 650 Ma (Merdith *et al.* 2017) for Pannotia formation and change in subduction pattern; (**e**) 600 Ma (Merdith *et al.* 2017) showing Pannotia formation and region of CIMP; (**f**) 550 Ma (Merdith *et al.* 2017) for Pannotia dispersal. S, Siberia; L, Laurentia; B, Baltica; A, Amazonia; CIMP, Central Iapetus Magmatic Province. In (c–e) convergence zones leading to the amalgamation of the Gondwanan portion of Pannotia (blue lines) correspond with the approximate location of subduction zones.

dated at *c.* 1.6–1.4 Ga (e.g. Pehrsson *et al.* 2015), Kenorland (Williams *et al.* 1991) thought to have existed during the interval *c.* 2.7–2.5 Ga, and possibly Ur (*c.* 3.0 Ga), although the latter is better described as a supercraton (i.e. transient, late Archean landmasses which broke up to form cratons, e.g. Bleeker 2003).

Although there are geological markers for supercontinent assembly (e.g. Nance *et al.* 2014), no formal system exists for supercontinent identification, as a result of which there is no formal definition of a supercontinent (e.g. Meert 2012). Even a basic understanding of how much contiguous landmass is required is open to debate. For example, Meert (2012) proposed a figure of 75% of available continent crust but, as pointed out by Nance and Murphy (2019), this is both difficult to estimate and views supercontinents as objects rather than the consequence of a geodynamic process.

The status of Pannotia (*c.* 0.65–0.54 Ga; Gondwana–Laurentia–Baltica and possibly Siberia, Fig. 1c–f), is an example of the ongoing debate about what constitutes a supercontinent (see Murphy *et al.* 2020; Evans, in press, this volume). Given the uncertainties inherent in Neoproterozoic palaeogeographical reconstructions, Nance and Murphy (2019) argue that Pannotia's status as a supercontinent is apparent from a number of 'supercontinent' markers around the time of its proposed formation (e.g. global-scale orogeny, rapid continental growth, profound changes in the chemistry of the oceans and atmosphere, rapid and dramatic climate swings, as well as an explosion in biological activity; Nance *et al.* 1986; Hoffman 1991; Hoffman *et al.* 1998; Maruyama and Santosh 2008; Knoll 2013). However, there is general agreement that Pannotia's size and duration were significantly less than that of Pangaea, drawing controversy as to whether it can be classified as a unique supercontinent or was simply part of Rodinia after initial break-up (e.g. Mitchell *et al.* 2012; Li *et al.* 2019).

An area of Pannotian dynamics that has not been fully explored is the response of the mantle to the continental convergence leading to its amalgamation. Late Neoproterozoic continental convergence and protracted subduction leading to the assembly of the Gondwanan portion of Pannotia is strongly indicated by widespread 'Pan-African' collisional orogenic activity between 0.62 and 0.53 Ga (e.g. Li *et al.* 2008; Merdith *et al.* 2017). Investigating the effect of continental convergence and assembly on Late Neoproterozoic–Early Paleozoic (0.6–0.5 Ga) mantle convection patterns, could allow for supercontinent identification through its impact on mantle dynamics (e.g. Heron 2019). Furthermore, as the legacy of such an impact would affect Paleozoic mantle convection patterns, it would also need to be factored into models purporting to explain the amalgamation of Pangaea.

The Central Iapetus Magmatic Province (CIMP, Fig. 1e, f) is one potential manifestation of changes in deep mantle circulation that may have been an outcome of continental convergence (in a similar way to the Central Atlantic Magmatic Province and the convergence of Pangaea). CIMP comprises several LIPs and predominantly consists of mafic dyke swarms, basalts, bimodal basalt–rhyolite complexes, lamprophyres and carbonatites (Kamo *et al.* 1995; Higgins and van Breemen 1998; Cawood *et al.* 2001; Puffer 2002; Keppie *et al.* 2006; Pisarevsky *et al.* 2008; Ernst and Bell 2010; Thomas *et al.* 2012; Ernst 2014). CIMP initiated along a rift–rift–rift triple junction between Laurentia, Baltica and Amazonia (Fig. 1e, f) with pulses of magmatism (peaking at *c.* 550 Ma) widely attributed to plumes that herald the opening of the Iapetus Ocean and Tornquist Sea (Cawood *et al.* 2001; Pisarevsky *et al.* 2008; Thomas *et al.* 2012).

In this study, we use 3D thermo-chemical global mantle convection experiments that take into account the palaeo-subduction history from Rodinia to Pangaea (Matthews *et al.* 2016; Merdith *et al.* 2017). We analyse the thermal response of the mantle driven by the evolution of surface tectonics to identify any mantle signatures generated by convergence leading to Pangaea and Rodinia assembly, and then apply these to Pannotia. The models are checked against geological markers such as plume and hotspot locations to gauge the influence of the convergence of continental material in influencing mantle dynamics.

Modelling global mantle convection

We model global mantle convection using the ASPECT code (Kronbichler *et al.* 2012; Heister *et al.* 2017). ASPECT solves the following set of equations for compressible convection in the Earth's mantle, describing the mass, momentum and energy balance (taking into account adiabatic heating, shear heating and radiogenic heat production), and the transport of chemical composition:

$$-\nabla \cdot (2\eta\dot{\varepsilon}) + \nabla p = \rho \mathbf{g}, \tag{1}$$

$$\nabla \cdot (\rho \mathbf{u}) = 0, \tag{2}$$

$$\rho C_{\mathrm{p}}\left(\frac{\partial T}{\partial t} + \mathbf{u}\cdot\nabla T\right) - \nabla\cdot k\nabla T = \rho H + 2\eta\dot{\varepsilon}:\dot{\varepsilon} + \alpha T(\mathbf{u}\cdot\nabla\rho), \tag{3}$$

$$\frac{\partial C}{\partial t} + \mathbf{u}\cdot\nabla C = 0 \tag{4}$$

The equations are solved for velocity $\boldsymbol{u}$, pressure p, temperature T and chemical composition C (e.g. harzburgite or recycled ocean crust). η is the viscosity, $\dot{\varepsilon} = \frac{1}{2}(\nabla\mathbf{u} + \nabla\boldsymbol{u}^{\boldsymbol{T}}) - \frac{1}{3}(\nabla\cdot\ \mathbf{u})\boldsymbol{\delta_{ij}}$ is the deviatoric strain rate, g is the gravitational acceleration, ρ is the density, C_{p} is the specific heat capacity (at constant pressure), k is the thermal conductivity, H is the radiogenic heat production and α is the thermal expansivity.

Our models begin from an initial condition that has an average mantle temperature gradient and composition that is appropriate for the present-day mantle (Fig. 2d) and in keeping with previous studies (e.g. Dannberg and Gassmöller 2018; Zhang and Li 2018). The initial mantle temperature is laterally homogeneous, following an adiabatic profile with thermal boundary layers at the top and bottom (Dannberg and Gassmöller 2018). We fix the surface temperature to 273 K and core–mantle boundary temperature to 3700 K (Fig. 2d). Although 3700 K is a higher temperature than some previous studies (e.g. Zhang and Li 2018), there is uncertainty in the exact value for the present day (e.g. Nomura *et al.* 2014). There is greater uncertainty in historical core-mantle temperature, with previous studies indicating a higher basal temperature in the Hadean (e.g. 4000 K, O'Neill and Zhang 2018). Here, by fixing the core–mantle boundary temperature throughout the study (from 1 Ga to 0 Ma), we do not capture the evolution of the interior average mantle temperature. However, the change in temperature between 1 Ga and the present day will not be significant given the uncertainty. As a result, a choice of 3700 K is appropriate for all geological times in the simulation.

Viscosity in the simulations (Fig. 2e) is depth- and temperature-dependent (as outlined in Heister *et al.* 2017) and based on a published viscosity model incorporating constraints from mineral

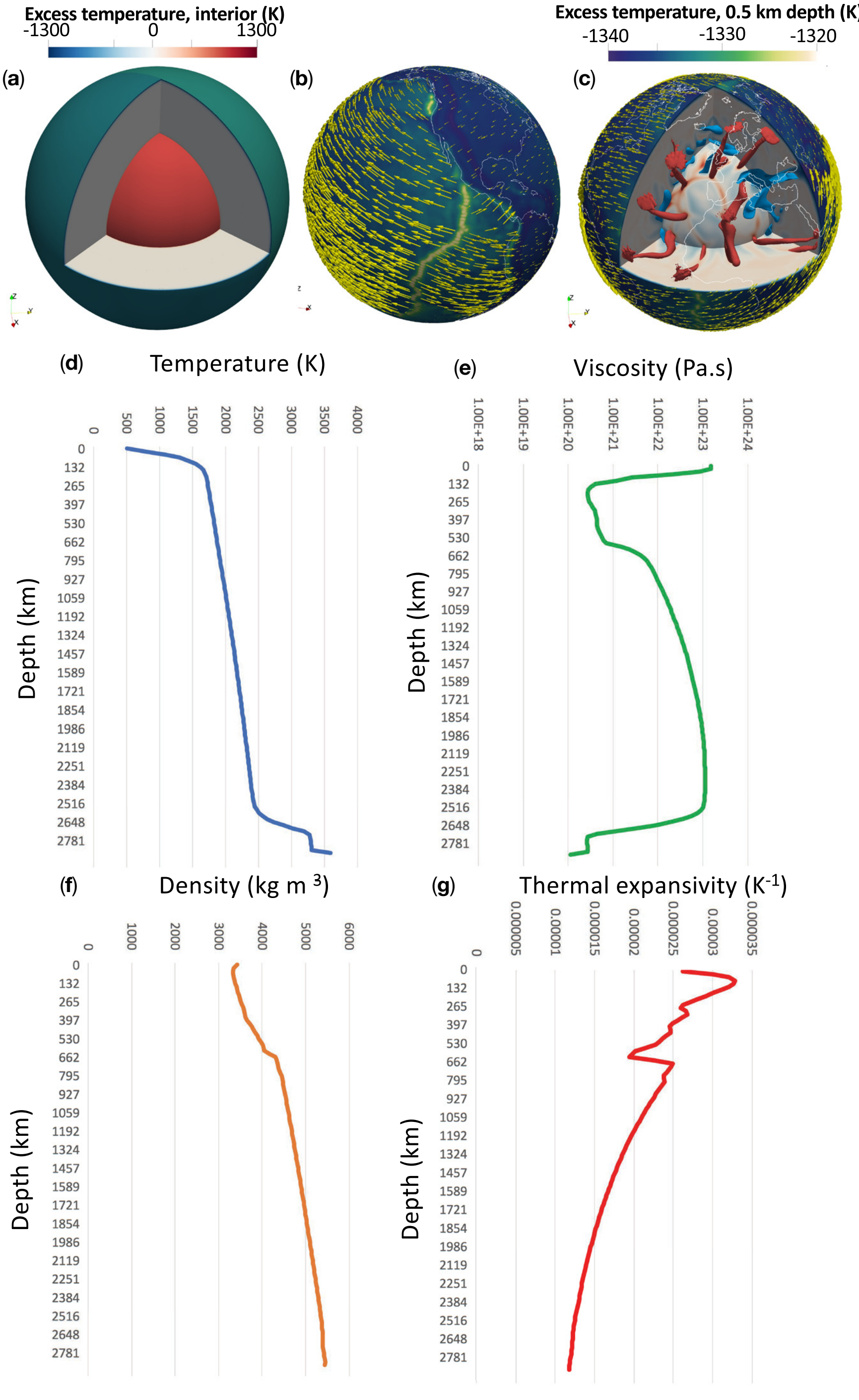

Fig. 2. The model setup. Global mantle convection models start from a homogenous initial condition (**a**) and are driven by plate velocities imposed at the surface (**b**) to produce subduction and (return-flow) plumes (**c**). The depth profiles of temperature (**d**), viscosity (**e**), density (**f**) and thermal expansivity (**g**) are given for the initial condition of a thermo-chemical model. The excess temperature is the difference between the temperature and adiabatic profiles (e.g. the non-adiabatic temperature).

physics, geoid deformation and seismic tomography (Steinberger and Calderwood 2006). Our model produces viscosity variations of four orders of magnitude over a temperature range appropriate for the Earth ($\Delta T = 3700$ K) (Fig. 2d). However, this viscosity range is manually limited to reduce the computation time and make model runs feasible. In the Earth, lateral viscosity contrasts are likely to be larger than in our models. As in previous studies (Dannberg and Gassmöller 2018), we assume an average mantle composition of 82% harzburgite and 18% recycled oceanic crust (Xu *et al.* 2008) and compute the material properties ρ, α and C_p using PerpleX (Connolly 2009) and a mineral physics database (Stixrude and Lithgow-Bertelloni 2011). Accordingly, all material properties include the effects of phase transitions, with thermal expansivity and specific heat taking into account the corresponding latent heat release and consumption (Nakagawa *et al.* 2009).

Although we do not prescribe continental and oceanic material present at the surface, the model uses temperature-dependent viscosity which form the outlines of plates bound by the ridges and subduction zones produced from the applied plate reconstruction velocities. In that respect, we can generate areas of reduced heat flux due to cold material thickening in response to plate tectonic processes. As a result, our models can act to produce areas of the surface that could be described as a 'continent' and 'ocean' (e.g. Fig. 3).

For this study, we used ASPECT version 2.0.0-pre (commit 572f967) but compared models with a more recent version of the code. This was done to ensure planned methodological changes to a new version of the global mantle convection setup used here did not impact the conclusions drawn from our (older) simulations. All model parameters are given in Table 1, and the initial radial profiles of temperature- and depth-dependent material properties are plotted in Figure 2.

The boundary condition at the surface is provided by plate reconstructions (Fig. 2b) and is therefore kinematic (e.g. it does not change in accordance with the force balance of the underlying mantle) (Fig. 2c). In this study we use two different plate reconstructions which produce (using GPlates 2.0) surface velocities at 1 myr intervals at a resolution of 1° × 1°. For our set of Pangaea models, we use the Matthews *et al.* (2016) plate reconstructions, which extend back in time 410 million years. The Matthews *et al.* (2016) global model includes the Paleozoic model of Domeier and Torsvik (2014) and the Mesozoic–Cenozoic model of Müller *et al.* (2016). For our set of Rodinia/Pannotia models, we use Merdith *et al.* (2017) plate reconstructions that cover the interval 1000 to 520 Ma (480 myr in total). Although these reconstructions do not yield a coherent Pannotia supercontinent, we utilize the surface velocity fields during the convergence that culminated in the Pan-African collisional orogenies and the assembly of Gondwana. At present, a plate reconstruction history between 0.52 and 0.41 Ga is not available, therefore we could not use a single simulation from 1 Ga to the present day.

We apply a 190 myr 'spin-up' period to the start of all models to reduce the impact of the initial condition on mantle dynamics. In starting our models from a spherically symmetrical setup (e.g. Fig. 2), there is a period where the mantle overturns – generating a pulse in core–mantle boundary heat flux. By applying a 'spin-up' phase of 190 myr, we ensure no signal from the initialization of the model affects our results. The time 190 myr was chosen as it is long enough that the mantle is well mixed but not so long that the models become 'expensive' to run on a supercomputer (i.e. slow). In model development, 50, 100 and 190 myr spin-up phases were tested – the overall trends of the heat flux in the models were similar in all cases ensuring the results were robust. The simulations last more than 600 myr in total, but our analysis begins after 190 myr when the mantle is well mixed. Further details of the model setup can be found in Dannberg and Gassmöller (2018).

In the following sections we describe the mantle dynamics that occur for two separate models: *Model PangT*, which uses 410 myr of surface velocities from the Matthews *et al.* (2016) plate reconstruction; and *Model NeoproT,* which applies surface velocities from the Merdith *et al.* (2017) plate reconstruction for 1000 to 520 Ma. Both models are purely thermal simulations, meaning there are no thermochemical piles present. We first look at the behaviour of the mantle in response to the formation and dispersal of the supercontinent Pangaea (e.g. *Model PangT)*, and then apply these responses to Pannotia to see whether this putative supercontinent can be identified from the evolution of the Neoproterozoic mantle (*Model NeoproT*).

The response of the mantle to supercontinent Pangaea

Studies analysing the timing of continent–continent collisions and age of rifting sequences show that the land masses of Gondwana (the African, Antarctic, India, Australian and South American plates) and Laurasia (the Eurasian and North American plates) formed the supercontinent Pangaea near the equator at *c.* 320 Ma (Smith *et al.* 1981; Hoffman 1991; Scotese 2001). The break-up of Pangaea is thought to have occurred in a number of stages with North America separating from the land mass at *c.* 180 Ma (starting the opening of the Central Atlantic Ocean), the dispersal of the Antarctic–Australian,

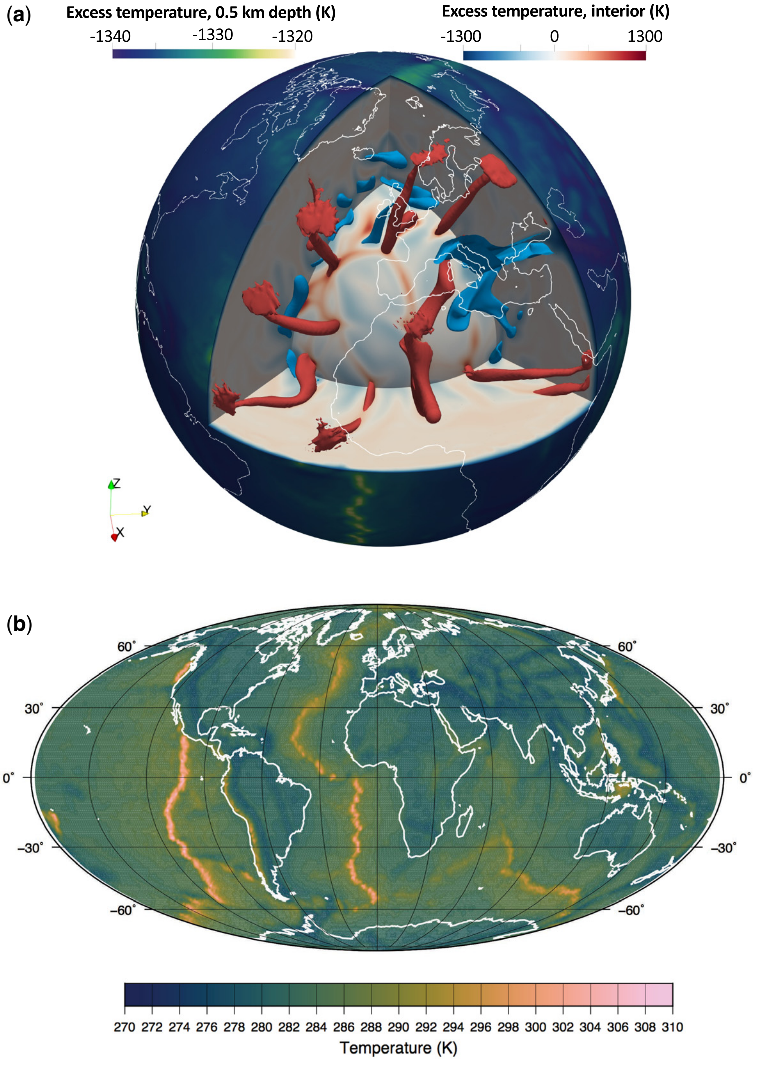

Fig. 3. Output of *Model PangT* for the present day (0 Ma). (**a**) A view into the mantle beneath the northern Atlantic and Europe for *Model PangT*. Excess mantle temperature anomaly contoured surfaces are given for warm (300 K, red) and cold (− 500 K, blue) regions. (**b**) Temperature at 1 km depth from the surface for the model, highlighting the present-day ridges and continents (continental outline shown by white lines, Matthews *et al.* 2016).

Indian and South American continents occurring between 140 and 100 Ma (Smith *et al.* 1981; Scotese 2001) and, finally, Australia separating from Antarctica during the Paleocene (Veevers and McElhinny 1976).

The surface velocities from Matthews *et al.* (2016) span 410 myr (410–0 Ma) and therefore encapsulate the formation and breakup of Pangaea. Although there is no continental material specified at the surface, our models apply appropriate subduction zone positions over time dictated by the plate reconstruction history. Figure 3 shows the output for *Model PangT* at 0 Ma (present day), with plumes rising from the core–mantle boundary to the surface alongside cold downwelling slabs interacting with the mantle flow (Fig. 3a). The temperature close to the surface shows the presence of ridges in appropriate positions in the mid-Atlantic, east Pacific, and Indian oceans for the present day (Fig. 3b).

Figure 4 shows the positioning of plumes over time for *Model PangT*. Plumes are calculated as areas with an excess temperature greater than 400 K at 700 km depth (shown in orange on Fig. 4). The hottest regions of plume activity are

Table 1. *Model material parameters*

Symbol	Variable	Value
η	Dynamic viscosity	5×10^{19}–1.5×10^{23}Pa s[b]
ρ	Density	3.3–5.8 g cm^{-3} (PerpleX[a])
g	Gravitational acceleration	9.81 m s^{-2}
C_p	Specific heat capacity	1058–1250 J kg^{-1} K^{-1} (PerpleX[a])
K	Thermal conductivity	4.7 W m^{-1} · K^{-}
H	Radiogenic heat production	6×10^{-12} W kg^{-1}
α	Thermal expansivity	0.65–3.6×10^{-5} K^{-1} (PerpleX[a])

[a]Connolly (2009); Stixrude & Lithgow-Bertelloni (2011); Xu *et al.* (2008).
[b]Steinberger and Calderwood (2006).

shown in red (>550 K). In our model, there are more plumes forming in regions where continental material would be located during supercontinent formation (7 red plumes in Fig. 4d) than there are during dispersal (3–4 in Fig. 4a, b). At 40 Ma in *Model PangT* (Fig. 4b), plumes form in the location of Iceland and the High Arctic, consistent with geological evidence (e.g. White and McKenzie 1989; Jones *et al.* 2002; Rickers *et al.* 2013). Likewise, during continental dispersal, a number of plumes are positioned along the mid-Atlantic ridge. There is also a distinct change in mantle dynamics from Pangaea formation to dispersal with plumes appearing to be mostly 'hot' (>550 K) (Fig. 4).

At 0 Ma (Fig. 4a), there is some agreement (and some disagreement) between the location of model plumes and the present-day hotspot database (Steinberger 2000; French and Romanowicz 2015). In particular, plumes form near the hotspots of Iceland, Hawaii, Samoa, Louisville, San Fernandez, Tristan, the Azores, Cameroon, and the East African Rift System. In testing the robustness of the simulation, we formally analysed the positioning of the hot thermal anomalies. For half the database *Model PangT* produces a plume within 1500 km of a present-day hotspot. This is a performance that is better than 80% of 10 000 simulations that randomly position the same number of plumes as *Model Pang T* (45) and then compare these to the 29 hotspots in the database.

By analysing the core–mantle boundary heat flux (Fig. 5a), we find a signature in the response of the mantle to the formation of the supercontinent Pangaea: the basal heat flux (e.g. core–mantle boundary) increases from 16 to 18 terawatt (TW) while Pangaea is contiguous (e.g. 320–180 Ma, Fig. 1a) and remains relatively stable (*c.* 18 TW) during dispersal (*c.* 180 Ma). It should be noted that the actual values given in our simulations for heat flux are strongly related to assumptions regarding lower mantle rheology. For example, changing the core–mantle temperature or thermal conductivity in the model would strongly influence the actual heat flux values – but not the overall trend.

Our models infer that convergence leading to Pangaea amalgamation may have been sufficient by 400 Ma to impact core–mantle boundary heat flux, as shown by the increase in Figure 5a. This timing corresponds to the 100 Ma record of convergence leading to the collision of promontories of Gondwana with Laurussia, a major phase in the amalgamation of Pangaea (e.g. Kroner and Romer 2013; Arenas *et al.* 2014; Wu *et al.* 2020). Since our global mantle convection *Model PangT* performs well against plume location tests (Fig. 4), we can apply the model's mantle response to Pangaea (Fig. 5a) to Neoproterozoic time to investigate whether Rodinia and/or Pannotia display a similar signature.

Pannotia's mantle signature?

Figures 5c, d, 6 and 7 show the response of the mantle to imposed surface velocities spanning 1000 to 520 Ma (Merdith *et al.* 2017). Based on the criteria specified in the previous section, we can identify the assembly and dispersal of Rodinia from the core–mantle boundary heat flux. Figure 5c shows the increase in heat flux during the assembly and lifespan of Rodinia – an increase which stops during its break-up and dispersal. A similar pattern of increasing basal heat flux is produced in our model between *c.* 660 and 570 Ma (Fig. 5c), which corresponds to continental convergence leading to the Pan-African collisions during which Pannotia is thought to have assembled. This increase stops post-570 Ma, with our model producing an increase in plume coverage (Fig. 5d). This timing corresponds with peak activity of CIMP. Some of the plumes form under the site of the putative supercontinent Pannotia at 550 Ma (Figs 6 & 7a).

The potential role of large low shear velocity provinces

Large structures of low shear-wave seismic velocities (large low shear velocity provinces or LLSVPs)

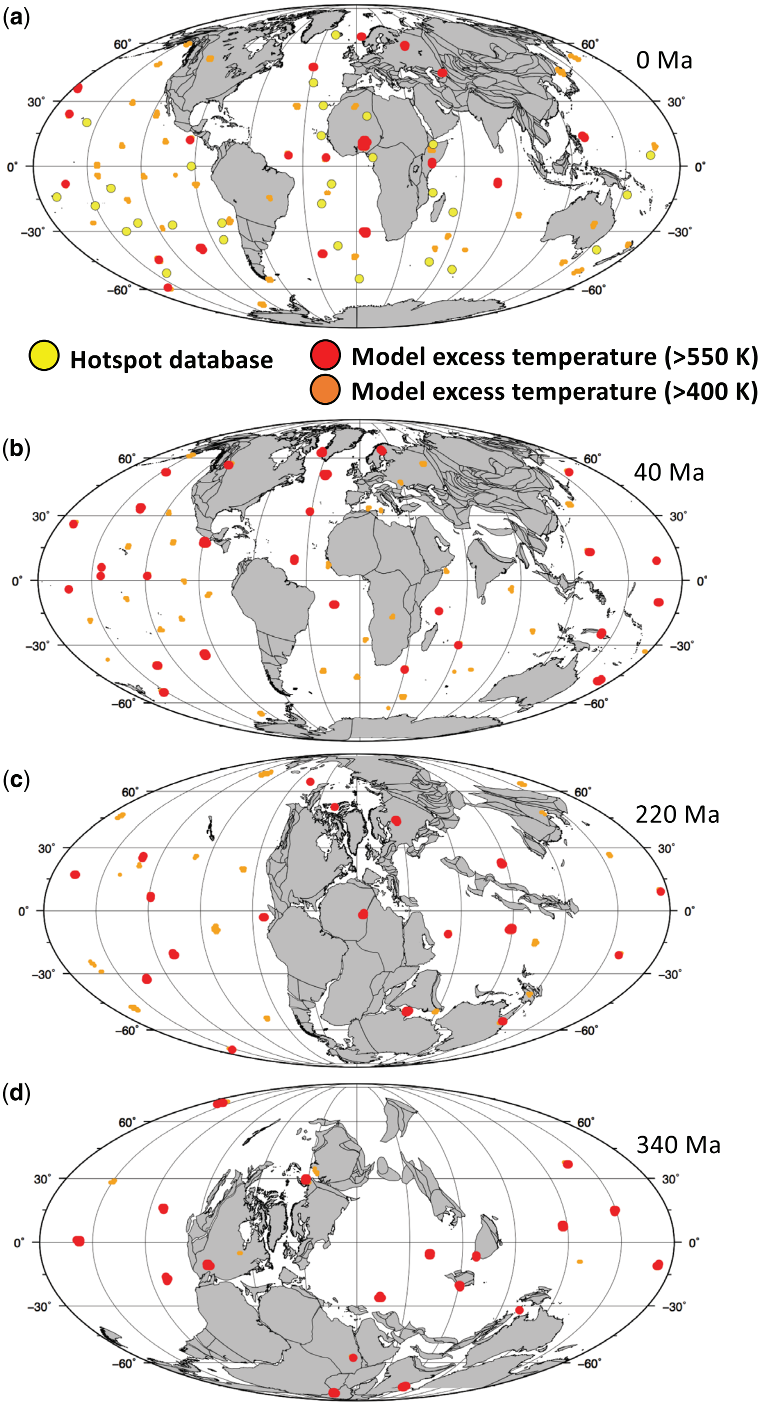

Fig. 4. Evolution of plume positions for *Model PangT* for the past 340 million years. (**a**) present day, (**b**) 40 Ma, (**c**) 220 Ma and (**d**) 340 Ma. Figures show continental positions as given by Matthews *et al.* (2016) and the plume positions at 700 km depth represented by excess temperature values of >550 K (red) and >400 K (orange). Present-day hotspot locations from French and Romanowicz (2015) and Steinberger (2000) are shown in yellow circles in (a).

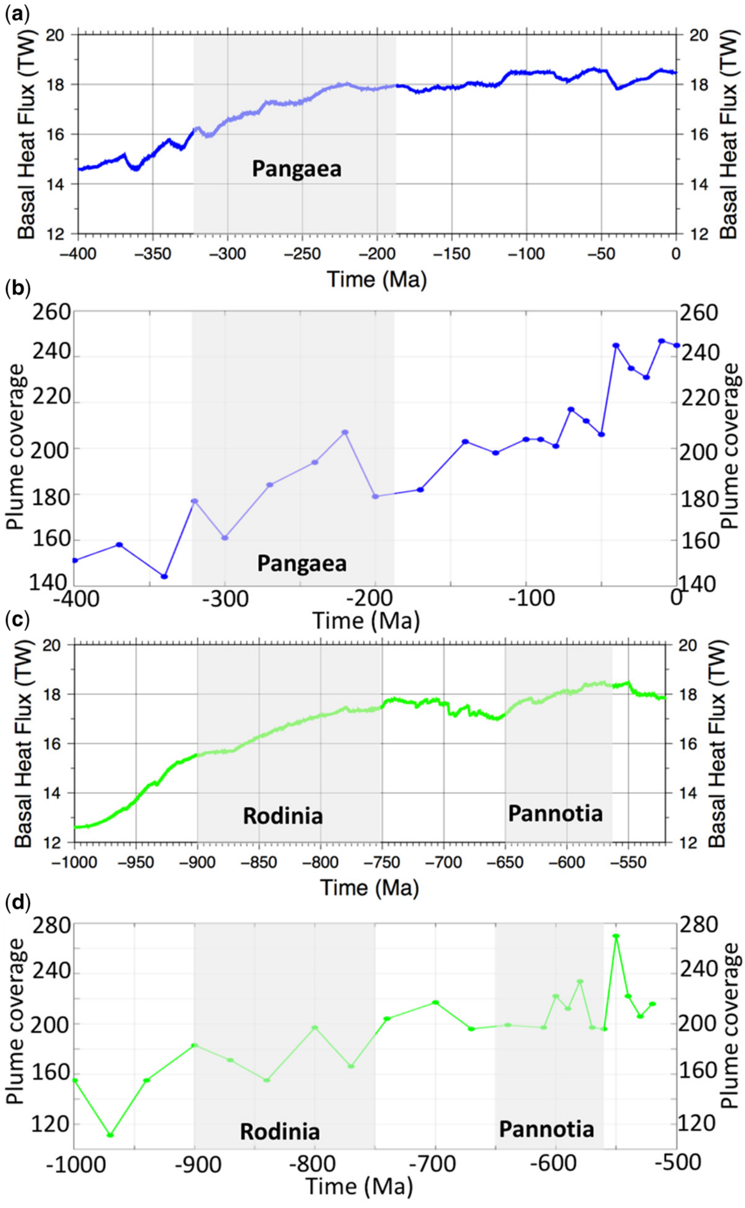

Fig. 5. Thermal response of the mantle to supercontinent formation and dispersal. (**a**) and (**c**) show the basal heat flux for *Model PangT* and *Model NeoproT*, respectively. Panels (**b**) and (**d**) show the evolution of plume coverage over time for the two models. Plume coverage is defined by the number of 1° × 1° boxes that have an excess temperature value >400 K at 700 km depth (e.g. a hot thermal anomaly). For example, at 400 Ma in (b), *Model PangT* has approximately 150 1° × 1° boxes that feature a 'plume' (which represents 0.5% of the potential coverage available). Times when a supercontinent may have been in existence are given by the shaded regions (Smith *et al.* 1981; Hoffman 1991; Scotese 2001; Li *et al.* 2008, 2013; Li and Evans 2011; Nance and Murphy 2019). The significant difference between the basal heat flux and plume coverage values for the end of *Model NeoproT* (520 Ma) as compared to the beginning of *Model PangT* (410 Ma) is an artefact of the two models using separate (non-continuous) plate reconstructions and beginning from different initial conditions.

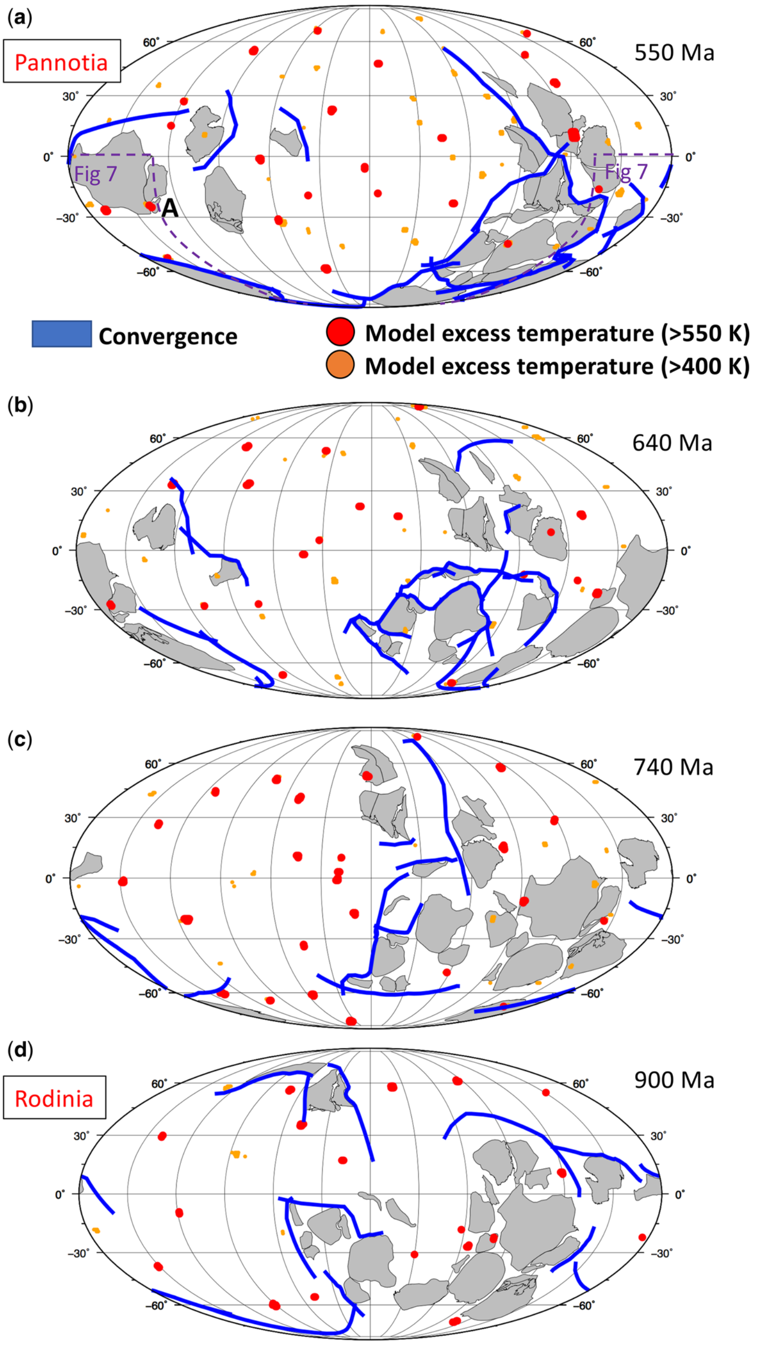

Fig. 6. Evolution of plume positions for *Model NeoproT* for the interval 900–550 Ma. (**a**) 550 Ma, (**b**) 640 Ma, (**c**) 740 Ma and (**d**) 900 Ma. Figures show continental and convergence locations as given by Merdith *et al.* (2017) and the plume positions at 700 km depth represented by excess temperature values of >550 K (red) and >400 K (orange). Dashed purple lines in (a) outline region displayed in Figure 7. Marker A is used as a reference for plume location in Figure 7a.

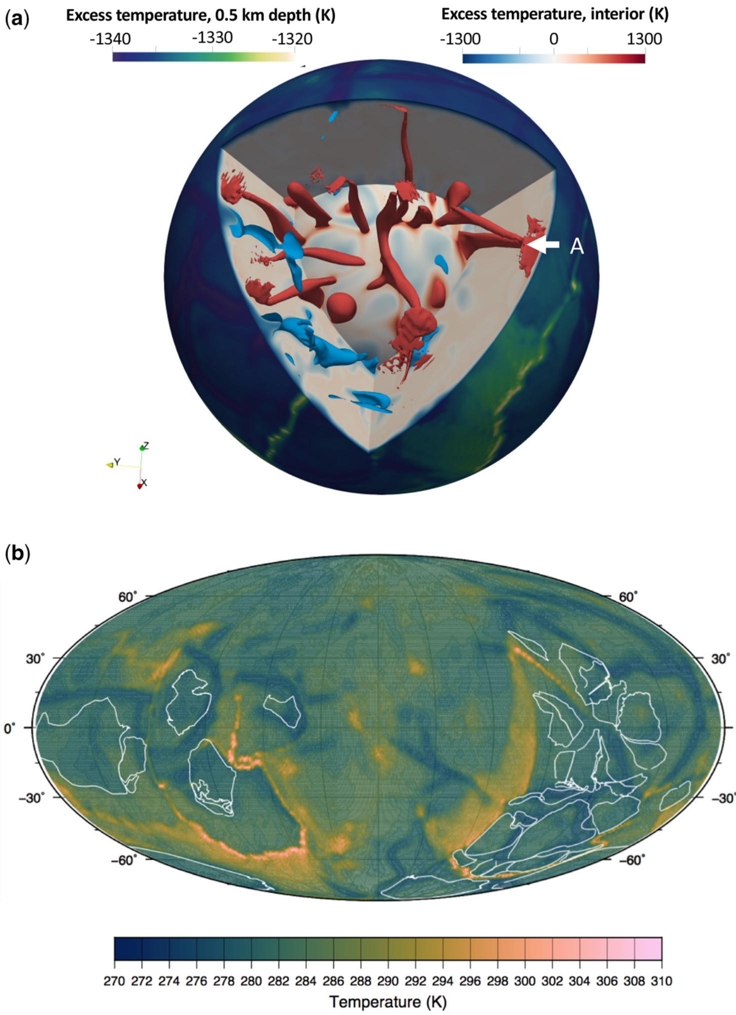

Fig. 7. Output of *Model NeoproT* post-Pannotia (550 Ma). (**a**) A view into the mantle in the area outlined in Figure 6a. Excess mantle temperature anomaly contoured surfaces are given for warm (300 K, red) and cold (− 500 K, blue) regions. Marker A is in reference to the plume location in Figure 6a. (**b**) Temperature at 1 km depth from the surface for the model, highlighting the position of ridges and continents (continental outline at 550 Ma from Merdith *et al.* 2017 shown in white).

observed in the lower mantle by seismic tomography studies and interpreted as regions of elevated temperatures and/or compositional anomaly, appear to play a defining role in the origin and positioning of mantle plumes (Steinberger 2000; Torsvik *et al.* 2006; Zhong *et al.* 2007; Deschamps *et al.* 2012; French and Romanowicz 2015; Cottaar and Lekic 2016). Although the composition and origin of LLSVPs are debated (e.g. Davies *et al.* 2012; Koelemeijer *et al.* 2017; Zaroli *et al.* 2017), there is growing consensus (Tan *et al.* 2002; Torsvik *et al.* 2006; Garnero *et al.* 2016) that plumes may form within or adjacent to these regions. In turn, the formation of plumes can influence supercontinent dispersal, leading to a further repositioning of subduction zones and a change in the pattern of mantle flow (van Hinsbergen *et al.* 2011). The relative importance of LLSVPs in controlling the positioning of mantle plumes is also controversial. The end-members of this debate are (i) that LLSVPs are spatially stable antipodal structures over time, with plumes generated from their edges (e.g. Torsvik *et al.* 2006, 2010), or that (ii) LLSVPs are entirely passive in mantle convection processes controlled by subduction flow (e.g. McNamara and

Zhong 2005; Zhong *et al.* 2007; Davies *et al.* 2012; Heron *et al.* 2015). The uncertainty and ambiguity in whether these geophysical features signify a dense, chemically distinct layer in the deep mantle (e.g. a thermo-chemical pile) or represent purely thermal anomalies make modelling mantle convection difficult (for reviews see Garnero *et al.* 2016; McNamara 2019).

The previous two models (*PangT* and *NeoproT*) do not feature any thermo-chemical layer. However, in *Model NeoproTC* we apply a 150 km thick thermo-chemical layer to the initial condition of the model (Fig. 2g). Following a number of previous studies (e.g. Heister *et al.* 2017; Dannberg and Gassmöller 2018), our model LLSVPs have the composition of mid-ocean ridge basalt and are therefore chemically distinct from the surrounding mantle. Here, the thermo-chemical piles have a corresponding buoyancy number $B = \Delta\rho/\alpha\rho\Delta T = 1.9$, where $\Delta\rho$ is the density contrast between the anomalously dense material and the average mantle composition and ΔT is the difference between the actual core–mantle boundary temperature (fixed at 3700 K) and the adiabatic profile (at a reference depth of 2500 km). Although the thermo-chemical pile has a higher density than the adjacent mantle, the layer is not fixed in one location and has the potential to move in response to mantle flow generated by subduction. After the 190 myr 'spin-up' period, the thermo-chemical material has been shaped by the mantle flow and is no longer in its initial position of a uniform layer at the core–mantle boundary.

Figure 8 shows the evolution of the thermo-chemical pile in *Model NeoproTC* from an initial uniform layer. The yellow colours outline the shape of the model LLSVP at 550 Ma with material located mainly in the present-day positions of the western Pacific Ocean, the Atlantic Ocean and Europe. Model plumes, given by the red markers, are generated mainly from the edges of the thermo-chemical piles rather than their interior (Fig. 8a). However, some plumes form at a distance from the thermo-chemical pile.

In comparison to the purely thermal model (*NeoproT*, Fig. 6a), the thermo-chemical simulation produces fewer hot plumes (red) under the oceanic lithosphere, although plumes still develop beneath similar continental locations (Fig. 8a). This simulation suggests that the overall pattern of plume formation is not significantly affected by the presence of a thermo-chemical layer (e.g. Hassan *et al.* 2015). Furthermore, the presence of a thermo-chemical layer acts as an insulator to the core, reducing the heat flow through the boundary (Fig. 8b).

In analysing the criteria for identifying a supercontinent, the basal heat flux in the presence of a thermo-chemical layer masks the dispersal of Rodinia and the formation of Pannotia. In *Model NeoproTC,* the core–mantle boundary heat flux continues to increase from 750 to 650 Ma (Fig. 8b), but in *Model NeoproT* it stabilized over the same time interval (Fig. 5c). However, the impact of the convergence leading to Pannotia assembly can still be identified at 650 Ma through the increased rate of heat leaving the core into the mantle. In terms of plume coverage, the evolution of *Model NeoproTC* (Fig. 8c) is similar to that of *NeoproT* (Fig. 5d): while Rodinia is being assembled there is an increase in plume coverage that stops following Rodinia break-up, but increases once more during the continental convergence leading to Pannotia. Due to the presence of a thermo-chemical pile, there is a larger plume coverage in *Model NeoproTC* than *NeoproT*.

A number of previous studies have proposed that LLSVPs may have been relatively fixed in their location on timescales greater than that of supercontinent formation and dispersal (Torsvik *et al.* 2006, 2010). Although spatially fixed thermo-chemical piles are not modelled in this study, we show the outline of present-day LLSVPs in Figure 8a to highlight where (potentially) a thermo-chemical pile would have been located with respect to Pannotia's continental configuration. The break-up of Pannotia could have been facilitated by mantle plumes forming at the edges of fixed LLSVPs, since Baltica, Siberia and southwestern Gondwana are situated above the margins of the present-day seismic anomalies. However, a number of plumes in both *Model NeoproTC* and *NeoproT* do form at what would be the edge of a present-day LLSVP location (e.g. markers 1–7, Fig. 8a), although no thermo-chemical piles are situated in the present-day positions.

Discussion

We developed 3D global mantle convection models that feature surface velocities linked to plate reconstructions to identify a mantle signature of supercontinent convergence, assembly and dispersal. By analysing the response of the mantle to the convergence, assembly and dispersal of Pangaea (410–0 Ma), we were able to identify such a signature, which we then compared with that of Rodinia and with convergence leading to assembly of hypothesized supercontinent Pannotia (620–540 Ma). For Pangaea and Rodinia, the models produce an increase in heat flux across the core–mantle boundary during the lifespan of the supercontinent (Fig. 5), and a stabilization in basal heat flux following break-up. For convergence leading to Pannotia assembly, the models produced a similar thermal response at the base of the mantle over similar timescales (Fig. 5).

These supercontinent 'markers' of core–mantle boundary heat flux and sub-continental plume formation (i.e. deep mantle convection patterns) are

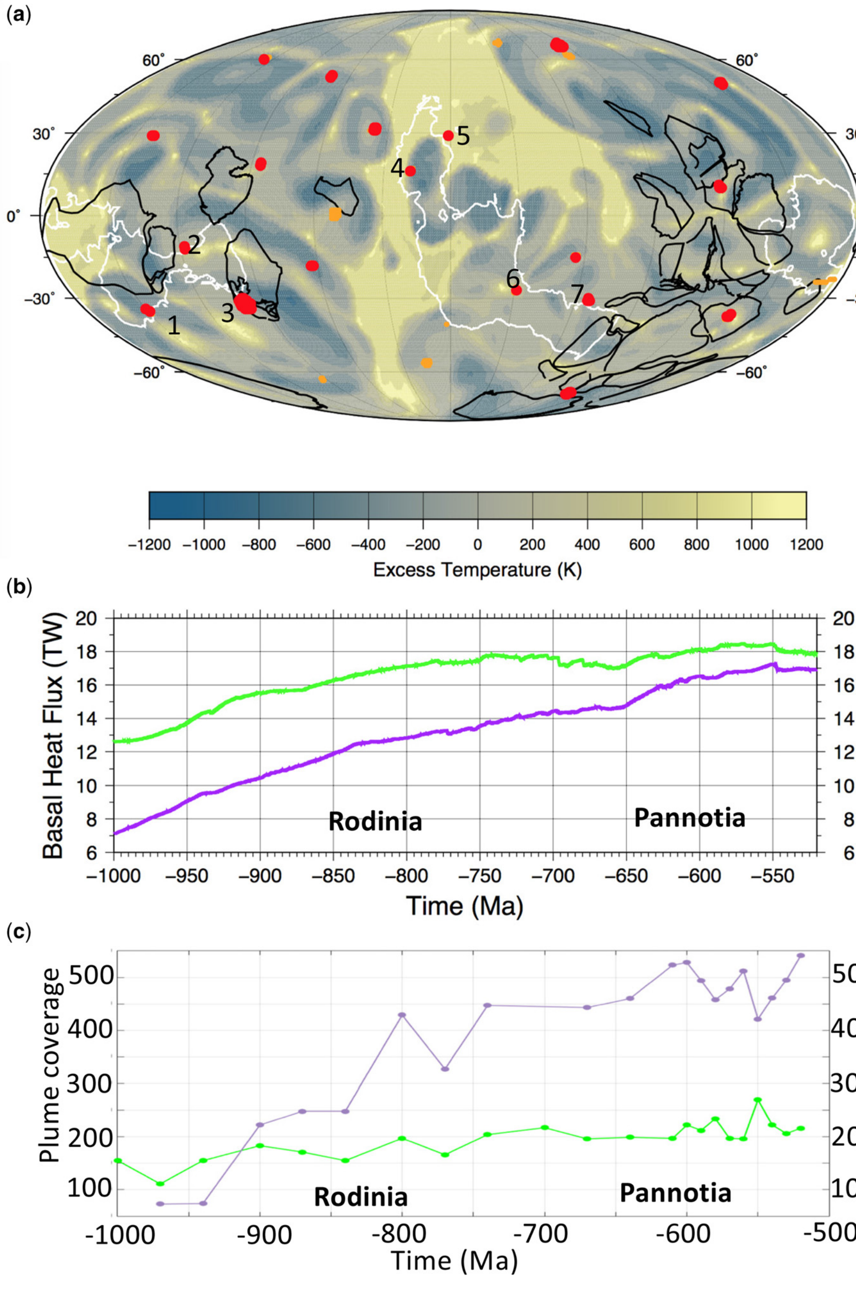

Fig. 8. Output of *Model NeoproTC* post-Pannotia (550 Ma). (**a**) Excess temperature of *Model NeoproTC* near the core-mantle boundary (2800 km depth) showing the outline of the thermo-chemical pile (yellow) alongside model plume positions (red and orange) and paleo-continent locations (black outline, Merdith *et al.* 2017). The white contour corresponds to the present-day positions of large low shear velocity provinces. This low velocity contour is generated from runs where 9 out of 14 seismic tomography models agree that there are slow anomalies (Shephard *et al.* 2017). Numbers 1 to 7 indicate model deep mantle plumes that originate close to the edge of present-day LLSVPs (white). Projection is centred on Greenwich Meridian. (**b**) Basal heat flux and (**c**) evolution of plume coverage for *Model NeoproTC* (purple) and *Model NeoproT* (green). Due to the presence of a thermo-chemical pile, there is a larger plume coverage in *Model NeoproTC* than *NeoproT*. Numbers 1 to 7 indicate model deep mantle plumes that originate close to the edge of present-day LLSVPs (white).

difficult to quantify in a geological context. However, there is a potential link between geomagnetic variations and mantle convection (e.g. Davies 1999; Buffett 2002). Simulations of the geodynamo suggest that transitions from periods of rapid polarity reversals to periods of prolonged stability (e.g. geomagnetic superchrons) may have been triggered by changes in core–mantle boundary heat flow either globally or in equatorial regions – a response that has been previously applied to the supercontinent cycle (e.g. Olson *et al.* 2010, 2015; Zhang and Zhong 2011; Biggin *et al.* 2012; Choblet *et al.* 2016). Our results are in agreement with previous studies that have applied similar methodologies. Zhang and Zhong (2011) used 3D numerical simulations and 450 myr of plate reconstruction history to analyse core–mantle boundary heat flux during supercontinent formation and dispersal. Despite generating very similar trends to this study for Pangaean heat flux with and without thermo-chemical piles, Zhang and Zhong (2011) highlighted the fluctuating heat flux between 100 Ma and the present day as being most important. The trend of increasing heat flux between 350 and 250 Ma (Fig. 5) that we present here is also shown in Zhang and Zhong (2011).

Our study marks a first step in the classification of periods of continental convergence and amalgamation over geological time through identifying mantle thermal responses to the convergence, assembly and dispersal stages of supercontinents. We do not model continental material which, in itself, has an impact on mantle dynamics through modifying the wavelength of mantle flow (Grigné *et al.* 2007; Phillips *et al.* 2009; Rolf *et al.* 2012) and the initiation and polarity of subduction (e.g. Crameri and Tackley 2014), alongside topographic and sea-level influences. However, we do prescribe surface velocities from plate reconstructions (Matthews *et al.* 2016; Merdith *et al.* 2017) that may help to artificially capture some aspects of these mantle dynamics. As a result, it would be possible to compare times of enhanced basal heat flux with the timing and frequency of orogenesis and potential sea-level variations, which are characteristics of supercontinent assembly (e.g. Nance and Murphy 2019). A study of the impact of our mantle convection models on crustal growth, climate, the evolution of life and biogeochemical cycles (i.e. other potential factors in supercontinent identification) would also be possible but is beyond the scope of this study. Although the models we present here do not take into consideration crustal growth (e.g. Hawkesworth *et al.* 2010; Rozel *et al.* 2017; Jain *et al.* 2019*a*, *b*), we do analyse the amount of plume coverage arriving from the deep mantle (e.g. Fig. 5). Such upwellings may help in understanding mantle circulation patterns over time when compared to the LIP record (Ernst *et al.* 2005; Ernst and Bleeker 2010).

The CIMP initiated along a rift–rift–rift triple junction between Laurentia, Baltica and Gondwana (Amazonia) and most reconstructions for the early stages of the opening of the Iapetus Ocean and Tornquist Sea invoke a plume centered on this triple junction (Higgins and van Breemen 1998; Cawood *et al.* 2001; Pisarevsky *et al.* 2008). In our numerical models a plume (and/or series of plumes) develops in the region where CIMP is thought to have originated (e.g. marker A in Figs 6a & 7a for *Model NeoproT*, and markers 1–3 in Fig. 8a for *Model NeoproTC*). Although we do not produce a suite of models that systematically test the potential density and rheology of the thermo-chemical layer at the base of the mantle, it is important to note that 'CIMP' plumes occur regardless of whether a model 'LLSVP' features in the models or not. This outcome indicates that the plate reconstruction history may play a more dominant role in mantle dynamics than the composition of the deep mantle (i.e. top-down over bottom-up), as previously proposed by McNamara and Zhong (2005) and Davies *et al.* (2012). The CIMP identification in our study can be used as an indication that the models are performing well. Future work to further analyse model LIPs during the timeframe of Pannotia will help us understand how robust such numerical models are in producing geological events.

The impact of continental insulation on the thermal evolution of our models cannot be assessed because the models do not include continental material. Nevertheless, some studies indicate that continental insulation is a potential driving mechanism for the supercontinent cycle. Given that Pangaea was relatively stable and largely stationary for >100 million years, Anderson (1982) proposed that continental insulation could have had a dramatic effect on the underlying mantle. Over this length of time, the excess heat trapped by the supercontinent would cause uplift (through thermal expansion), partial melting of the mantle and, ultimately, the dispersal of continental material (Anderson 1982; Worsley *et al.* 1984; Nance *et al.* 1986, 1988; Gurnis 1988). In addition, a large geoid high similar to that over present-day Africa would be generated sub-supercontinent as a result of the thermal expansion caused by the continental insulation. Subsequent numerical (e.g. Lowman and Jarvis 1993, 1999; Zhong and Gurnis 1993; Yoshida *et al.* 1999; Lenardic *et al.* 2005, 2011; Phillips and Bunge 2005; Coltice *et al.* 2007, 2009; Phillips *et al.* 2009; Phillips and Coltice 2010; Yoshida 2010; Rolf *et al.* 2012) and geochemical (Brandl *et al.* 2013; Brown and Johnson 2018) studies suggest an important role for continental insulation in producing increased sub-continental mantle temperatures.

Although the models presented here do not take into consideration continental insulation, there remains a thermal response to the formation of a supercontinent that generates elevated subcontinental temperatures (e.g. Fig. 5). However, we find that subduction history is the most important factor in driving mantle convection patterns; an observation that follows a number of previous studies that suggest a diminished role of continental insulation in global mantle dynamics (Lowman and Jarvis 1995, 1996; Heron and Lowman 2010, 2011, 2014; Yoshida 2013; Heron *et al.* 2015).

The results presented here represent a first step in understanding global mantle convection during the late Neoproterozoic. A comparison between different numerical methodologies would be beneficial to test the robustness of our findings. A better understanding of the role of the initial thermal condition in the generation of a mantle 'signal' in response to a supercontinent is also needed. Furthermore, we only use one interpretation of what the plate reconstruction history could have been during the Neoproterozoic. For instance, Scotese and Elling (2017) present reconstruction for the time period with a contiguous Pannotia. Given the difficulty in generating plate reconstructions at any given time period (let alone a billion years ago), we acknowledge the uncertainty surrounding the plate velocities used in our mantle convection models. Further work in this field must be used to contrast and compare the impact of different plate reconstructions on mantle convection models.

The availability of a plate reconstruction history between 0.52 and 0.41 Ga could be used to produce a single simulation covering a billion years, rather than the two separate models for 1 to 0.52 Ga (Merdith *et al.* 2017) and 0.41 Ga to the present day (Matthews *et al.* 2016) that we implement. Future work that incorporates a full plate reconstruction history from 1 Ga to the present day would allow for a better understanding of the transition between supercontinent dispersal and formation, in particular for Pangaea. In the models presented here, there is a significant difference between the basal heat flux and plume coverage values for the end of *Model NeoproT* (520 Ma, Fig. 5c, d) as compared to the beginning of *Model PangT* (410 Ma, Fig. 5a, b). This difference is an artefact of the two models using separate (non-continuous) plate reconstructions and beginning from different initial conditions.

Our models indicate that the convergence, assembly and dispersal of Pannotia had a mantle response that we can measure. However, it is unlikely that the continental extent of Pannotia would fulfil the criterion that a supercontinent should consist of at least 75% of the preserved continental crust prior to initial breakup (Meert 2012). To test further the robustness of our models, it would be appropriate to compare the thermal evolution of the mantle from numerical simulations that do not feature prescribed plate surface velocities (e.g. Phillips *et al.* 2009; Phillips and Coltice 2010; Rolf and Tackley 2011; Rolf *et al.* 2012, 2014, 2018). By allowing the surface to evolve dynamically, rather than kinematically (e.g. McNamara and Zhong 2005; Heron and Lowman 2010, 2011, 2014; Davies *et al.* 2012; Heron *et al.* 2015; Li and Zhong 2017), the mantle interior is not 'forced' into particular mantle convection patterns. Modelling with dynamic boundary conditions could provide further information on the level of continental amalgamation needed to generate a 'significant' mantle response, and whether or not a 'small' supercontinent can generate a global geodynamics signature (as shown here).

Conclusions

We present the first 3D global mantle convection models aimed at identifying a thermal response to the formation of Pannotia. By analysing the mantle signature of the amalgamation of Pangaea and Rodinia (Figs 4 & 6), we find that an increase in core–mantle boundary heat flux and plume formation may be markers of a supercontinent (Fig. 5). Our results suggest that the convergence, assembly and dispersal of Pannotia had a thermal legacy that needs to be applied to models of Pangaea amalgamation. Such a legacy is not factored into models of tectonic evolution in which the transition from Rodinia to Pangaea represents one supercontinent cycle (Murphy *et al.* 2020). This thermal signature occurs in our numerical models during the time of Pannotia, indicating that such a continental amalgamation may have the ability to impact mantle dynamics (Fig. 5). This finding is supported by the development of plumes in the spatial and temporal location of the Central Iapetus Magmatic Province (CIMP). However, our findings are inconclusive on the potential role of large low shear velocity provinces (LLSVPs) in the development of plumes and subsequent break-up of supercontinents (Fig. 8). We did not find a significant difference in the plume locations and mantle dynamics of numerical simulations with and without thermo-chemical piles.

The results here represent an important contribution to a growing body of research that is posing questions on the fundamentals of global mantle convection: how do we define a supercontinent? In this initial study, we show that the formation of Pannotia generates an identifiable change in mantle flow, in line with processes related to the (less controversial) supercontinents of Pangaea and Rodinia. Here, we posit that identifying the mantle response to a supercontinent is key to formalizing a definition. This thermal signature occurs in our models during the time of continental convergence leading to Pannotia amalgamation, indicating that such a continental convergence may have had the ability to impact mantle dynamics (Fig. 5).

Acknowledgements We thank reviewers Sergei Pisarevsky and Tobias Rolf for their insightful comments which led to significant improvements in the manuscript. This paper is part of UNESCO IGCP Project 648: Supercontinent Cycles and Global Geodynamics. Computations were performed on the Niagara supercomputer at the SciNet HPC Consortium (Loken *et al.* 2010).

Funding PJH is grateful for funding from a Marie Skłodowska Curie Actions Individual Fellowship, proposal 749664. JBM acknowledges the continuing support of N.S.E.R.C. Canada (A06223) and RDN acknowledges support provided by Project CZ.02.2.69/0.0/0.0/16_015/0002362 of the Czech Operational Programme Research, Development and Education. SciNet is funded by the Canada Foundation for Innovation; the Government of Ontario; Ontario Research Fund-Research Excellence; and the University of Toronto. We thank the Computational Infrastructure for Geodynamics (geodynamics.org) which is funded by the National Science Foundation under award EAR-0949446 and EAR-1550901 for supporting the development of ASPECT.

Author contributions **PJH**: data curation (lead), formal analysis (equal), funding acquisition (lead), investigation (lead), methodology (lead), project administration (lead), software (lead), validation (lead), visualization (lead), writing – original draft (equal); **JBM**: conceptualization (equal), formal analysis (equal), investigation (equal), writing – original draft (equal); **RDN**: conceptualization (equal), formal analysis (equal), investigation (equal), writing – original draft (equal); **RNP**: formal analysis (equal), funding acquisition (equal), resources (lead), writing – original draft (lead).

Data availability statement Data and input files related to the numerical modelling of the paper will be made available at https://github.com/heronphi/Heron_Pannotia. A number of figures in this manuscript were generated using Generic Mapping Tools (Wessel *et al.* 2013) and applying Scientific Colour Maps (Crameri 2018).

References

Anderson, D.L. 1982. Hotspots, polar wander, Mesozoic convection and the geoid. *Nature*, **297**, 391–393, https://doi.org/10.1038/297391a0

Arenas, R., Díez Fernández, R., Sánchez Martínez, S., Gerdes, A., Fernández-Suárez, J. and Albert, R. 2014. Two-stage collision: exploring the birth of Pangaea in the Variscan terranes. *Gondwana Research*, **25**, 756–763, https://doi.org/10.1016/j.gr.2013.08.009

Biggin, A.J., Steinberger, B. *et al.* 2012. Possible links between long-term geomagnetic variations and whole-mantle convection processes. *Nature Geoscience*, **5**, 526–533, https://doi.org/10.1038/ngeo1521

Bleeker, W. 2003. The late Archean record: a puzzle in ca. 35 pieces. *Lithos*, **71**, 99–134, https://doi.org/10.1016/j.lithos.2003.07.003

Brandl, P.A., Regelous, M., Beier, C. and Haase, K.M. 2013. High mantle temperatures following rifting caused by continental insulation. *Nature Geoscience*, **6**, 391–394. https://doi.org/10.1038/NGEO1758

Brown, M. 2007. Metamorphism, plate tectonics, and the supercontinent cycle. *Earth Science Frontiers*, **14**, 1–18, https://doi.org/10.1016/S1872-5791(07)60001-3

Brown, M. and Johnson, T. 2018. Secular change in metamorphism and the onset of global plate tectonics, *American Mineralogist*, **103**, 181–196, https://doi.org/10.2138/am-2018-6166

Buffett, B.A. 2002. Estimates of heat flow in the deep mantle based on the power requirements for the geodynamo. *Geophysical Research Letters*, **29**, 1566. https://doi.org/10.1029/2001GL014649

Cawood, P.A., McCausland, P.J.A. and Dunning, G.R. 2001. Opening Iapetus: constraints from the Laurentian margin in Newfoundland. *Geological Society of America Bulletin*, **113**, 443–453, https://doi.org/10.1130/0016-7606(2001)113<0443:OICFTL>2.0.CO;2

Choblet, G., Amit, H. and Husson, L. 2016. Constraining mantle convection models with palaeomagnetic reversals record and numerical dynamos. *Geophysical Journal International*, **207**, 1165–1184, https://doi.org/10.1093/gji/ggw328

Coltice, N., Phillips, B.R., Bertrand, H., Ricard, Y. and Rey, P. 2007. Global warming of the mantle at the origin of flood basalts over supercontinents. *Geology*, **35**, 391–394, https://doi.org/10.1130/G23240A.1

Coltice, N., Herve, B., Rey, P., Jourdan, F., Phillips, B.R. and Ricard, Y. 2009. Global warming of the mantle beneath continents back to the Archaean. *Gondwana Research*, **15**, 254–266, https://doi.org/10.1016/j.gr.2008.10.001

Condie, K.C. 2011. *The Supercontinent Cycle. Earth as an Evolving Planetary System*. Academic Press, San Diego, CA.

Connolly, J.A.D. 2009. The geodynamic equation of state: what and how. *Geochemistry, Geophysics, Geosystems*, **10**, 1–19, https://doi.org/10.1029/2009GC002540

Cottaar, S. and Lekic, V. 2016. Morphology of seismically slow lower-mantle structures. *Geophysical Journal International*, **207**, 1122–1136, https://doi.org/10.1093/gji/ggw324

Courtillot, V., Jaupart, C., Manighetti, I., Taponier, P. and Besse, J. 1999. On causal links between flood basalts and continental breakup. *Earth and Planetary Science Letters*, **166**, 177–195, https://doi.org/10.1016/S0012-821X(98)00282-9

Crameri, F. and Tackley, P.J. 2014. Spontaneous development of arcuate single-sided subduction in global 3-D mantle convection models with a free surface. *Journal of Geophysical Research: Solid Earth*, **119**, 5921–5942, https://doi.org/10.1002/2014JB010939

Crameri, F. 2018. Geodynamic diagnostics, scientific visualisation and StagLab 3.0. *Geoscientific Model Development*, **11**, 2541–2562, https://doi.org/10.5194/gmd-11-2541-2018

Dalziel, I.W.D. 1991. Pacific margins of Laurentia and East Antarctica–Australia as a conjugate rift pair: evidence and implications for an Eocambrian supercontinent. *Geology*, **19**, 598–560, https://doi.org/10.1130/0091-7613(1991)019<0598:PMOLAE>2.3.CO;2

Dannberg, J. and Gassmöller, R. 2018. Chemical trends in ocean islands explained by plume–slab interaction. *Proceedings of the National Academy of Sciences*, **115**, 4351–4356, https://doi.org/10.1073/pnas.1714125115

Davies, G.F. 1999. *Dynamic Earth: Plates, Plumes and Mantle Convection*. Cambridge University Press, Cambridge

Davies, R.D., Goes, S., Davies, J.H., Schuberth, B.S.A., Bunge, H.-P. and Ritsema, J. 2012. Reconciling dynamic and seismic models of Earth's lower mantle: the dominant role of thermal heterogeneity. *Earth and Planetary Science Letters*, **353–354**, 253–269, https://doi.org/10.1016/j.epsl.2012.08.016

Deschamps, F., Cobden, L. and Tackley, P.J. 2012. The primitive nature of large low shear-wave velocity provinces. *Earth and Planetary Science Letters*, **349–350**, 198–208. https://doi.org/10.1016/j.epsl.2012.07.012

Domeier, M. and Torsvik, T.H. 2014. Plate tectonics in the late Paleozoic. *Geoscience Frontiers*, **5**, 303–350, https://doi.org/10.1016/j.gsf.2014.01.002

Ernst, R.E. 2014. *Large Igneous Provinces*. Cambridge University Press, Cambridge.

Ernst, R.E. and Bell, K. 2010. Large igneous provinces (LIPs) and carbonatites. *Mineralogy and Petrology*, **98**, 55–76, https://doi.org/10.1007/s00710-009-0074-1

Ernst, R.E. and Bleeker, W. 2010. Large igneous provinces (LIPs), giant dyke swarms, and mantle plumes: significance for breakup events within Canada and adjacent regions from 2.5 Ga to the Present. *Canadian Journal of Earth Sciences*, **47**, 695–739, https://doi.org/10.1139/E10-025

Ernst, R.E., Buchan, K.L. and Campbell, I.H. 2005. Frontiers in Large Igneous Province research. *Lithos*, **79**, 271–297, https://doi.org/10.1016/j.lithos.2004.09.004

Evans, D.A.D., In press. Pannotia under prosecution. *In*: Murphy, J.B., Strachan, R.A. & Quesada, C. (eds) 2020. *Pannotia to Pangaea: Neoproterozoic and Paleozoic Orogenic Cycles in the Circum-Atlantic Region*. Geological Society, London, Special Publications, **503**, https://doi.org/10.1144/SP503-2020-182

French, S.W. and Romanowicz, B. 2015. Broad plumes rooted at the base of the earth's mantle beneath major hotspots. *Nature*, **525**, 95–99, https://doi.org/10.1038/nature14876

Gamal El Dien, H., Doucet, L.S. and Li, Z. 2019, Global geochemical fingerprinting of plume intensity suggests coupling with the supercontinent cycle. *Nature Communications*, **10**, 5270, https://doi.org/10.1038/s41467-019-13300-4

Garnero, E.J., McNamara, A.K. and Shim, S.-H. 2016. Continent-sized anomalous zones with low seismic velocity at the base of earth's mantle. *Nature Geoscience*, **9**, 481–489, https://doi.org/10.1038/ngeo2733

Goldfarb, R.J., Bradley, D.C. and Leach, D.L. 2010. Secular variation in economic geology. *Economic Geology*, **105**, 459–465, https://doi.org/10.2113/gsecongeo.105.3.459

Grigné, C., Labrosse, S., Tackley, P. 2007. Convection under a lid of finite conductivity in wide aspect ratio models: effect of continents on the wavelength of mantle flow. *Journal of Geophysical Research*, **112**, 1–14, https://doi.org/10.1029/2006JB004297

Gurnis, M. 1988. Large-scale mantle convection and the aggregation and dispersal of supercontinents. *Nature*, **332**, 695–699, https://doi.org/10.1038/332695a0

Hassan, R., Flament, N., Gurnis, M., Bower, D.J. & Müller, D. 2015. Provenance of plumes in global convection models. *Geochemistry, Geophysics, Geosystems* **16**, 1465–1489, http://dx.doi.org/10.1002/2015GC005751

Hawkesworth, C.J., Dhuime, B., Pietranik, A.B., Cawood, P.A., Kemp, A.I.S. and Storey, C.D. 2010. The generation and evolution of the continental crust. *Journal of the Geological Society, London*, **167**, 229–248, https://doi.org/10.1144/0016-76492009-072

Hawkesworth, C.J., Cawood, P.A. and Dhuime, B. 2016. Tectonics and crustal evolution. *Geological Society of America: Today*, **26**, 4–11, https://doi.org/10.1130/GSATG272A.1

Heister, T., Dannberg, J., Gassmöller, R. and Bangerth, W. 2017. High accuracy mantle convection simulation through modern numerical methods. II: realistic models and problems. *Geophysical Journal International*, **210**, 833–851, https://doi.org/10.1093/gji/ggx195

Heron, P.J. 2019. Mantle plumes and mantle dynamics in the Wilson Cycle. *Geological Society, London, Special Publications*, **470**, 87–103, https://doi.org/10.1144/SP470.18

Heron, P.J. and Lowman, J.P. 2010.Thermal response of the mantle following the formation of a "super-plate". *Geophysical Research Letters*, **37**, 1–4, https://doi.org/10.1029/2010GL045136

Heron, P.J. and Lowman, J.P. 2011. The effects of supercontinent size and thermal insulation on the formation of mantle plumes. *Tectonophysics*, **510**, 28–38, https://doi.org/10.1016/j.tecto.2011.07.002

Heron, P.J. and Lowman, J.P. 2014. The impact of Rayleigh number on assessing the significance of supercontinent insulation. *Journal of Geophysical Research: Solid Earth*, **119**, 711–733, https://doi.org/10.1002/2013JB010484

Heron, P.J., Lowman, J.P. and Stein, C. 2015. Influences on the positioning of mantle plumes following supercontinent formation. *Journal of Geophysical Research Solid Earth*, **120**, 3628–3648, https://doi.org/10.1002/2014JB011727

Higgins, M.D. and van Breemen, O. 1998. The age of the Sept Iles layered mafic intrusion, Canada: implications for the Late Neoproterozoic/Cambrian history of Southeastern Canada. *Journal of Geology*, **106**, 421–431, https://doi.org/10.1086/516033

Hoffman, P.F. 1991. Did the breakout of Laurentia turn Gondwanaland inside-out? *Science*, **252**, 1409–1412, https://doi.org/10.1126/science.252.5011.1409

Hoffman, P.F. 1997. Tectonic genealogy of North America. *In*: Van der Pluijm, B.A. and Marshak, S. (eds) *An Introduction to Structural Geology and Tectonics*. McGraw-Hill, New York, 459–464.

Hoffman, P.F., Kaufman, A.J., Halverson, G.P. and Schrag, D.P. 1998. A Neoproterozoic snowball Earth. *Science*, **281**, 1342–1346, https://doi.org/10.1126/science.281.5381.1342

Jain, C., Rozel, A.B., Tackley, P.J., Sanan, P. and Gerya, T. 2019*a*. Growing primordial continents self-consistently in global mantle convection models. *Gondwana Research*, **73**, 96–122, https://doi.org/10.1016/j.gr.2019.03.015

Jain, C., Rozel, A.B. and Tackley, P.J. 2019*b*. Quantifying the correlation between mobile continents and elevated temperatures in the subcontinental mantle. *Geochemistry, Geophysics, Geosystems*, **20**, 1358–1386, https://doi.org/10.1029/2018GC007586

Jones, A.P., Price, G.D., Pricea, N.J., DeCarli, P.S. and Clegg, R.A. 2002. Impact induced melting and the development of large igneous provinces. *Earth and Planetary Science Letters*, **202**, 551–561, https://doi.org/10.1016/S0012-821X(02)00824-5

Kamo, S.L., Krogh, T.E. and Kumarapeli, P.S. 1995. Age of the Grenville dyke swarm, Ontario- Quebec: implications for the timing of Iapetan rifting. *Canadian Journal of Earth Sciences*, **32**, 273–280, https://doi.org/10.1139/e95-022

Keppie, J.D., Dostal, J., Nance, R.D., Miller, B.V., Ortega-Rivera, A. and Lee, J.K.W. 2006. Ca. 546 Ma plume-related dykes in the ∼1 Ga Novillo Gneiss (east-central Mexico): evidence for the initial separation of Avalonia. *Precambrian Research*, **147**, 342–353, https://doi.org/10.1016/j.precamres.2006.01.020

Knoll, A.H. 2013. Systems paleobiology. *Geological Society of America Bulletin*, **125**, 3–13, https://doi.org/10.1130/B30685.1

Koelemeijer, P., Deuss, A. and Ritsema, J. 2017. Density structure of earth's lowermost mantle from stoneley mode splitting observations. *Nature Communications*, **8**, 15241. https://doi.org/10.1038/ncomms15241

Kronbichler, M., Heister, T. and Bangerth, W. 2012. High accuracy mantle convection simulation through modern numerical methods. *Geophysical Journal International*, **191**, 12–29, https://doi.org/10.1111/j.1365-246X.2012.05609.x

Kroner, U. and Romer, R.L. 2013. Two plates – Many subduction zones: the Variscan orogeny reconsidered. *Gondwana Research*, **24**, 298–329, https://doi.org/10.1016/j.gr.2013.03.001

Lenardic, A., Moresi, L.-N., Jellinek, A.M. and Manga, M. 2005. Continental insulation, mantle cooling, and the surface area of oceans and continents. *Earth and Planetary Science Letters*, **234**, 317–333, https://doi.org/10.1016/j.epsl.2005.01.038

Lenardic, A., Moresi, L.-N., Jellinek, A.M., O'Neill, C., Cooper, C.M. and Lee, C.T. 2011, Continents, supercontinents, mantle thermal mixing, and mantle thermal isolation: theory, numerical simulations, and laboratory experiments. *Geochemistry, Geophysics, Geosystems*, **12**, 1–23, https://doi.org/10.1029/2011GC003663

Li, Z.X. and Evans, D.A.D. 2011. Late Neoproterozoic 40° intraplate rotation within Australia allows for a tighter-fitting and longer-lasting Rodinia. *Geology*, **39**, 39–42, https://doi.org/10.1130/G31461.1

Li, Z.X. and Zhong, S. 2009. Supercontinent–superplume coupling, true polar wander and plume mobility: plate dominance in whole-mantle tectonics. *Physics of the Earth and Planetary Interiors*, **176**, 143–156, https://doi.org/10.1016/j.pepi.2009.05.004

Li, Z.X. and Zhong, S. 2017. The source location of mantle plumes from 3D spherical models of mantle convection. *Earth and Planetary Science Letters*, **478**, 47–57, https://doi.org/10.1016/j.epsl.2017.08.033

Li, Z.X., Evans, D.A.D. and Zhang, S. 2004. A 90° Spin on Rodinia: possible causal links between the Neoproterozoic supercontinent, superplume, true polar wander and low latitude glaciation. *Earth and Planetary Science Letters*, **220**, 409–421, https://doi.org/10.1016/S0012-821X(04)00064-0

Li, Z.X., Bogdanova, S.V. *et al*. 2008. Assembly, configuration, and break-up history of Rodinia: a synthesis. *Precambrian Research*, **160**, 179–210, https://doi.org/10.1016/j.precamres.2007.04.021

Li, Z.X., Evans, D.A.D. and Halverson, G.P. 2013. Neoproterozoic glaciations in a revised global palaeogeography from the breakup of Rodinia to the assembly of Gondwanaland. *Sedimentary Geology*, **294**, 219–232, https://doi.org/10.1016/j.sedgeo.2013.05.016

Li, Z.X., Mitchell, R.N., Spencer, C.J., Ernst, R., Pisarevsky, S., Kirscher, U. and Murphy, J.B. 2019. Decoding Earth's rhythms: modulation of supercontinent cycles by longer superocean episodes. *Precambrian Research*, **323**, 1–5. https://doi.org/10.1016/j.precamres.2019.01.009

Lindsay, J.F. and Brasier, M.D. 2002. Did global tectonics drive early biosphere evolution? Carbon isotope record from 2.6 to 1.9 Ga carbonates of Western Australian basins. *Precambrian Research*, **114**, 1–34, https://doi.org/10.1016/S0301-9268(01)00219-4

Loken, C., Gruner, D. *et al*. 2010. Scinet: lessons learned from building a power-efficient top-20 system and data centre. *Journal of Physics: Conference Series*, **256**, 1–35, https://doi.org/10.1088/1742-6596/256/1/012026

Lowman, J.P. and Jarvis, G.T. 1993. Mantle convection flow reversals due to continental collisions. *Geophysical Research Letters*, **20**, 2087–2090, https://doi.org/10.1029/93GL02047

Lowman, J.P. and Jarvis, G.T. 1995. Mantle convection models of continental collisions and breakup incorporating finite thickness plates. *Physics of the Earth and Planetary Interiors*, **88**, 53–68, https://doi.org/10.1016/0031-9201(94)05076-A

Lowman, J.P. and Jarvis, G.T. 1996. Continental collisions in wide aspect ratio and high Rayleigh number two-dimensional mantle convection models. *Journal of Geophysical Research*, **101**, 25 485–25 497, https://doi.org/10.1029/96JB02568

Lowman, J.P. and Jarvis, G.T. 1999, Effects of mantle heat source distribution on continental stability. *Journal of Geophysical Research*, **104**, 12 733–12 746, https://doi.org/0148-0227/99/1999JB900108509

Maruyama, S. and Santosh, M. 2008. Models on Snowball Earth and Cambrian explosion: a synopsis. *Gondwana Research*, **14**, 22–32, https://doi.org/10.1016/j.gr.2008.01.004

Matthews, K., Maloney, K., Zahirovic, S., Williams, S., Seton, M. and Müller, R.D. 2016. Global plate boundary evolution and kinematics since the late Paleozoic. *Global and Planetary Change*, **146**, 226–250, https://doi.org/10.1016/j.gloplacha.2016.10.002

McNamara, A.K. 2019. A review of large low shear velocity provinces and ultra-low velocity zones. *Tectonophysics*, **760**, 199–220, https://doi.org/10.1016/j.tecto.2018.04.015

McNamara, A.K. and Zhong, S.J. 2005. Thermochemical structures beneath Africa and the Pacific Ocean. *Nature*, **437**, 1136–1139, https://doi.org/10.1038/nature04066

Meert, J.G. 2012. What's in a name? The Columbia (Paleopangaea/Nuna) supercontinent. *Gondwana Research*, **21**, 987–993, https://doi.org/10.1016/j.gr.2011.12.002

Melezhik, V.A., Kump, L.R., Hanski, E.J., Fallick, A.E. and Prave, A.R. 2013. Tectonic evolution and major global earth-surface palaeoenvironmental events in the Palaeoproterozoic. *In*: Melezhik, V., Prave, A.R., Fallick, A.E., Kump, L.R., Strauss, H., Lepland, A. and Hanski, E.J. (eds) *Reading the Archive of Earth's Oxygenation. Vol. 1: The Palaeoproterozoic of Fennoscandia as Context for the Fennoscandian Arctic Russia – Drilling Early Earth Project*. Springer, Berlin, 3–21.

Merdith, A.S., Collins, A.S. *et al*. 2017. A full-plate global reconstruction of the Neoproterozoic. *Gondwana Research*, **50**, 84–134, https://doi.org/10.1016/j.gr.2017.04.001

Mitchell, R.N., Kilian, T.M. and Evans, D.A.D. 2012, Supercontinent cycles and the calculation of absolute palaeolongitude in deep time. *Nature*, **482**, 208–211, https://doi.org/10.1038/nature10800

Moores, E.M. 1991. Southwest U.S.-East Antarctic (SWEAT) connection: a hypothesis. *Geology*, **19**, 425–428, https://doi.org/10.1130/0091-7613(1991)019<0425:SUSEAS>2.3.CO;2

Müller, R.D., Dutkiewicz, A., Seton, M. and Gaina, C. 2013. Seawater chemistry driven by supercontinent assembly, breakup, and dispersal. *Geology*, **41**, 907–910, https://doi.org/10.1130/G34405.1

Müller, R.D., Seton, M. *et al*. 2016. Ocean basin evolution and global-scale plate reorganization events since Pangea breakup. *Annual Reviews of Earth and Planetary Sciences*, **44**, 107–138, https://doi.org/10.1146/annurev-earth-060115-012211

Murphy, J.B., Nance, R.D. *et al*. 2020. *In*: Murphy, J.B., Strachan, R.A. and Quesada, C. (eds) *Pannotia to Pangaea: Neoproterozoic and Paleozoic Orogenic Cycles in the Circum-Atlantic Region*. Geological Society, London, Special Publications, **503**, https://doi.org/10.1144/SP503-2020-96

Nakagawa, T., Tackley, P.J., Deschamps, F. and Connolly, J.A.D. 2009. Incorporating self- consistently calculated mineral physics into thermochemical mantle convection simulations in a 3-d spherical shell and its influence on seismic anomalies in earth's mantle. *Geochemistry, Geophysics, Geosystems*, **10**, https://doi.org/10.1029/2008GC002280

Nance, R.D. and Murphy, J.B. 2013. Origins of the supercontinent cycle. *Geoscience Frontiers*, **4**, 439–448, https://doi.org/10.1016/j.gsf.2012.12.007

Nance, R.D. and Murphy, J.B. 2019. Supercontinents and the case for Pannotia. *In*: Wilson, R.W., Houseman, G.A., McCaffrey, K.J.W., Doré, A.G. and Buiter, S.J.H. (eds) *Fifty Years of the Wilson Cycle Concept in Plate Tectonics*. Geological Society, London, Special Publications, **470**, 65–85, https://doi.org/10.1144/SP470.5

Nance, R.D., Worsley, T.R. and Moody, J.B. 1986. Post-Archean biogeochemical cycles and long-term episodicity in tectonic processes. *Geology*, **14**, 514–518, https://doi.org/10.1130/0091-7613(1986)14<514:PBCALE>2.0.CO;2

Nance, R.D., Worsley, T.R. and Moody, J.B. 1988. The supercontinent cycle. *Scientific American*, **256**, 72–79, https://doi.org/10.1038/scientificamerican0788-72

Nance, R.D., Murphy, J.B. and Santosh, M. 2014. The supercontinent cycle: a retrospective essay. *Gondwana Research*, **25**, 4–29, https://doi.org/10.1016/j.gr.2012.12.026

Nomura, R., Hirose, K., Uesugi, K., Ohishi, Y., Tsuchiyama, A., Miyake, A. and Ueno, Y. 2014. Low core–mantle boundary temperature inferred from the solidus of pyrolite. *Science*, **343**, 522–525, https://doi.org/10.1126/science.1248186

Olson, P.L., Coe, R.S., Driscoll, P.E., Glatzmaier, G.A. and Roberts, P.H. 2010. Geodynamo reversal frequency and heterogeneous core–mantle boundary heat flow. *Physics of the Earth and Planetary Interiors*, **180**, 66–79, https://doi.org/10.1016/j.pepi.2010.02.010

Olson, P., Deguen, R., Rudolph, M. and Zhong, S. 2015. Core evolution driven by mantle global circulation. *Physics of the Earth and Planetary Interiors*, **243**, 44–55, https://doi.org/10.1016/j.pepi.2015.03.002

O'Neill, C.J. and Zhang, S. 2018. Lateral mixing processes in the Hadean. *Journal of Geophysical Research: Solid Earth*., **123**, 7074–7089, https://doi.org/10.1029/2018JB015698

Pehrsson, S.J., Eglington, B.M., Evans, D.A.D., Huston, D. and Reddy, S.M. 2015. Metallogeny and its link to orogenic style during the Nuna supercontinent cycle. *Geological Society, London, Special Publications*, **424**, 83–94, https://doi.org/10.1144/SP424.5

Phillips, B.R. and Bunge, H.-P. 2005. Heterogeneity and time dependence in 3D spherical mantle convection models with continental drift. *Earth and Planetary Science Letters*, **233**, 121–135, https://doi.org/10.1016/j.epsl.2005.01.041

Phillips, B.R. and Coltice, N. 2010. Temperature beneath continents as a function of continental cover and convective wavelength. *Journal of Geophysical Research*, **115**, https://doi.org/10.1029/2009JB006600

Phillips, B., Bunge, H.P. and Schaber, K. 2009. True polar wander in mantle convection models with multiple, mobile continents. *Gondwana Research*, **15**, 288–296, https://doi.org/10.1016/j.gr.2008.11.007

Pisarevsky, S.A., Murphy, J.B., Cawood, P.A. and Collins, A.S. 2008. Late Neoproterozoic and Early Cambrian palaeogeography: models and problems. *Geological Society, London, Special Publications*, **294**, 9–31, https://doi.org/10.1144/SP294.2

Puffer, J.H. 2002. A Late Neoproterozoic eastern Laurentian superplume: location, size, chemical composition, and environmental impact. *American Journal of Science*, **302**, 1–27, https://doi.org/10.2475/ajs.302.1.1

Rickers, F., Fichtner, A. and Trampert, J. 2013. The Iceland–Jan Mayen plume system and its impact on mantle dynamics in the North Atlantic region: evidence from full-waveform inversion. *Earth and Planetary Science Letters*, **367**, 39–51, https://doi.org/10.1016/j.epsl.2013.02.022

Rogers, J.J.W. and Santosh, M. 2002. Configuration of Columbia, a Mesoproterozoic supercontinent. *Gondwana Research*, **5**, 5–22, https://doi.org/10.1016/S1342-937X(05)70883-2

Rolf, T. and Tackley, P. 2011. Focussing of stress by continents in 3D spherical mantle convection with self-consistent plate tectonics. *Geophysical Research Letters*, **38**, L18301, https://doi.org/10.1029/2011GL048677

Rolf, T., Coltice, N. and Tackley, P. 2012. Linking continental drift, plate tectonics and the thermal state of the Earth's mantle. *Earth and Planetary Science Letters*, **351–352**, 134–146, https://doi.org/10.1016/j.epsl.2012.07.011

Rolf, T., Coltice, N. and Tackley, P. 2014. Statistical cyclicity of the supercontinent cycle. *Geophysical Research Letters*, **41**, 2351–2358, https://doi.org/10.1002/2014GL059595

Rolf, T., Capitanio, F. and Tackley, P. 2018. Constraints on mantle viscosity structure from spherical convection models of Earth's continental motion and configuration evolution. *Tectonophysics*, **746**, 339–351, https://doi.org/10.1016/j.tecto.2017.04.031

Rozel, A.B., Golabek, G.J., Jain, C., Tackley, P.J. and Gerya, T. 2017. Continental crust formation on early Earth controlled by intrusive magmatism. *Nature*, **545**, 332–335, https://doi.org/10.1038/nature22042

Santosh, M. 2010*a*. Assembling North China Craton within the Columbia supercontinent: the role of double-sided subduction. *Precambrian Research*, **178**, 149–167, https://doi.org/10.1016/j.precamres.2010.02.003

Santosh, M. 2010*b*. Supercontinent tectonics and biogeochemical cycle: a matter of 'life and death'. *Geoscience Frontiers*, **1**, 21–30, https://doi.org/10.1016/j.gsf.2010.07.001

Scotese, C.R. 2001. *Atlas of Earth History, 1*. Paleogeography, PALEOMAP Project, Arlington, Texas, p. 58.

Scotese, C.R. and Elling, R. 2017. Plate tectonic evolution during the last 1.3 billion years: the movie, William Smith Meeting 2017: Plate Tectonics at 50. 29 September –1 October 2017, Geological Society, London.

Shephard, G.E., Matthews, K.J., Hosseini, K. and Domeier, M. 2017. On the consistency of seismically imaged lower mantle slabs. *Scientific Reports*, **7**, 1–17, https://doi.org/10.1038/s41598-017-11039-w

Smith, A.G., Hurley, A.M. and Briden, J.C. 1981. *Phanerozoic Paleocontinental World Maps*. Cambridge University Press, Cambridge.

Sobolev, S., Sobolev, A. *et al*. 2011. Linking mantle plumes, large igneous provinces and environmental catastrophes. *Nature*, **477**, 312–316, https://doi.org/10.1038/nature10385

Steinberger, B. 2000. Plumes in a convecting mantle: models and observations for individual hotspots. *Journal of Geophysical Research: Solid Earth*, **105**, 11 127–11 152, https://doi.org/10.1029/1999JB900398

Steinberger, B. and Calderwood, A.R. 2006. Models of large-scale viscous flow in the earth's mantle with constraints from mineral physics and surface observations. *Geophysical Journal International*, **167**, 1461–1481, https://doi.org/10.1111/j.1365-246X.2006.03131.x

Strand, K. 2012. Global and continental-scale glaciations on the Precambrian earth. *Marine and Petroleum Geology*, **33**, 69–79, https://doi.org/10.1016/j.marpetgeo.2012.01.011

Stixrude, L. and Lithgow-Bertelloni, C. 2011. Thermodynamics of mantle minerals – ii. phase equilibria. *Geophysical Journal International*, **184**, 1180–1213, https://doi.org/10.1111/j.1365-246X.2010.04890.x

Tan, E., Gurnis, M. and Han, L. 2002. Slabs in the lower mantle and their modulation of plume formation. *Geochemistry, Geophysics, Geosystems*, **3**, 1067. https://doi.org/10.1029/2001GC000238

Thomas, W.A., Tucker, R.D., Astini, R.A. and Denison, R.E. 2012. Ages of pre-rift basement and synrift synrift?? rocks along the conjugate rift and transform margins of the Argentine Precordillera and Laurentia. *Geosphere*, **8**, 1366–1383, https://doi.org/10.1130/GES00800.1

Torsvik, T. 2003. The Rodinia jigsaw puzzle. *Science*, **300**, 1379–1381, https://doi.org/10.1126/science.1083469

Torsvik, T.H., Smethurst, M.A., Burke, K. and Steinberger, B. 2006. Large igneous provinces generated from the margins of the large low-velocity provinces in the deep mantle. *Geophysics Journal International*, **167**, 1447–1460, https://doi.org/10.1111/j.1365-246X.2006.03158.x

Torsvik, T.H., Burke, K., Steinberger, B., Webb, S.J. and Ashwal, L.D. 2010. Diamonds sampled by plumes from the core-mantle boundary. *Nature*, **466**, https://doi.org/10.1038/nature09216

van Hinsbergen, D.J.J., Steinberger, B., Doubrovine, P.V. and Gassmöller, R. 2011. Acceleration and deceleration of India–Asia convergence since the Cretaceous: roles of mantle plumes and continental collision. *Journal of Geophysical Research*, **116**, 1–20, https://doi.org/10.1029/2010JB008051

Veevers, J.J. and McElhinny, M.W. 1976. The separation of Australia from other continents. *Earth-Science Reviews*, **12**, 139–159, https://doi.org/10.1016/0012-8252(76)90003-9

Wessel, P., Smith, W.H.F., Scharroo, R., Luis, J.F. and Wobbe, F. 2013. Generic Mapping Tools: improved version released. *Eos, Transactions, American Geophysical Union*, **94**, 409–410, https://doi.org/10.1002/2013EO450001

White, R. and McKenzie, D. 1989. Magmatism at rift zones: the generation of volcanic continental margins and flood basalts. *Journal of Geophysical Research*, **94**, 7685–7729, https://doi.org/10.1029/JB094iB06p07685

Williams, H., Hoffman, P.F., Lewry, J.F., Monger, J.W.H. and Rivers, T. 1991. Anatomy of North America: thematic portrayals of the continent. *Tectonophysics*, **187**, 117–134, https://doi.org/10.1016/0040-1951(91)90416-P

Worsley, T.R., Nance, R.D. and Moody, J.B. 1984. Global tectonics and eustasy for the past 2 billion years. *Marine Geology*, **58**, 373–400, https://doi.org/10.1016/0025-3227(84)90209-3

Wu, L., Murphy, J.B., Quesada, C., Li, Z.-X., Waldron, J.W.F., Williams, S., Pisarevsky, S., and Collins, W.J. 2020. *The formation of Pangea: Paleomagnetic and geological observations revisited*. Geological Society of America Bulletin, https://doi-org.libproxy.stfx.ca/10.1130/B35633.1

Xu, W., Lithgow-Bertelloni, C., Stixrude, L. and Ritsema, J. 2008. The effect of bulk composition and temperature on mantle seismic structure. *Earth and Planetary Science Letters*, **275**, 70–79, https://doi.org/10.1016/j.epsl.2008.08.012

Yale, L.B. and Carpenter, S.J. 1998. Large igneous provinces and giant dike swarms: proxies for supercontinent cyclicity and mantle convection. *Earth and Planetary Science Letters*, **163**, 109–122, https://doi.org/10.1016/S0012-821X(98)00179-4

Yoshida, M. 2010. Preliminary three-dimensional model of mantle convection with deformable, mobile continental lithosphere. *Earth and Planetary Science Letters*, **295**, 205–218. https://doi.org/10.1016/j.epsl.2010.04.001

Yoshida, M. 2013. Mantle temperature under drifting deformable continents during the supercontinent cycle, *Geophysical Research Letters*, **40**, 1–6, https://doi.org/10.1002/grl.50151

Yoshida, M., Iwase, Y. and Honda, S. 1999. Generation of plumes under a localized high viscosity lid in 3-D spherical shell convection. *Geophysical Research Letters*, **26**, 947–950, https://doi.org/10.1029/1999 GL900147

Young, G.M. 2012. Evolution of Earth's climatic system: Evidence from ice ages, isotopes, and impacts. *GSA Today*, **23**, 10, 4–10. https://doi.org/10.1130/GSATG183A.1

Zaroli, C., Koelemeijer, P. and Lambotte, S. 2017. Toward seeing the earth's interior through unbiased tomographic lenses. *Geophysical Research Letters*, **44**, 11 399–11 408, https://doi.org/10.1002/2017GL074996

Zhang, N. and Li, Z.-X. 2018. Formation of mantle "lone plumes" in the global downwelling zone – a multiscale modelling of subduction-controlled plume generation beneath the south china sea. *Tectonophysics*, **723**, 1–13, https://doi.org/10.1016/j.tecto.2017.11.038

Zhang, N. and Zhong, S. 2011. Heat fluxes at the Earth's surface and core–mantle boundary since Pangea formation and their implication for the geomagnetic superchrons, 2011. *Earth and Planetary Science Letters*, **306**, 205–216, https://doi.org/10.1016/j.epsl.2011.04.001

Zhong, S. and Gurnis, M. 1993. Dynamic feedback between a continent like raft and thermal convection. *Journal of Geophysical Research*, **98**, 12 219–12 232, https://doi.org/10.1029/93JB00193

Zhong, S.J., Zhang, N., Li, Z.X. and Roberts, J. 2007. Supercontinent cycles, true polar wander, and very long wavelength mantle convection. *Earth and Planetary Science Letters*, **375**, 115–122, https://doi.org/10.1016/j.epsl.2007.07.049